

Irreversible Inactivation of Glutathione Peroxidase 1 and Reversible Inactivation of Peroxiredoxin II by H₂O₂ in Red Blood Cells

Chun-Seok Cho,^{1,2} Sukmook Lee,¹ Geun Taek Lee,¹ Hyun Ae Woo,¹ Eui-Ju Choi,² and Sue Goo Rhee¹

Abstract

Catalase, glutathione peroxidase1 (GPx1), and peroxiredoxin (Prx) II are the principal enzymes responsible for peroxide elimination in RBC. We have now evaluated the relative roles of these enzymes by studying inactivation of GPx1 and Prx II in human RBCs. Mass spectrometry revealed that treatment of GPx1 with H₂O₂ converts the selenocysteine residue at its active site to dehydroalanine (DHA). We developed a blot method for detection of DHA-containing proteins, with which we observed that the amount of DHA-containing GPx1 increases with increasing RBC density, which is correlated with increasing RBC age. Given that the conversion of selenocysteine to DHA is irreversible, the content of DHA-GPx1 in each RBC likely reflects total oxidative stress experienced by the cell during its lifetime. Prx II is inactivated by occasional hyperoxidation of its catalytic cysteine to cysteine sulfinic acid during catalysis. We believe that the activity of sulfiredoxin in RBCs is sufficient to counteract the hyperoxidation of Prx II that occurs in the presence of the basal level of H₂O₂ flux resulting from hemoglobin autoxidation. If the H₂O₂ flux is increased above the basal level, however, the sulfinic Prx II begins to accumulate. In the presence of an increased H₂O₂ flux, inhibition of catalase accelerated the accumulation of sulfinic Prx II, indicative of the protective role of catalase. *Antioxid. Redox Signal.* 12, 1235–1246.

Introduction

HEME IRON IN DEOXYHEMOGLOBIN (deoxyHb) is in the ferrous state in red blood cells (RBCs). The binding of O₂ to heme iron results in electron delocalization, with the Fe(II)–O₂ bond being in equilibrium with the Fe(III)–superoxide anion (O₂^{•−}) bond (34, 43). Occasionally, the superoxide anion is released instead of oxygen, resulting in the autoxidation of Hb to metHb with iron in the ferric state, which cannot bind O₂. The superoxide anion is dismutated to H₂O₂, which can be further converted to the hydroxyl radical, and other hydroperoxides. In RBCs, the autoxidation of 3% of total Hb to metHb is estimated to occur each day (20, 42). Oxygen transport by RBCs is thus a substantial contributor to oxidative stress. RBCs are equipped with various antioxidant enzymes to cope with reactive oxygen species (ROS) produced as the result of the autoxidation of hemoglobin (Hb). Enzymes responsible for the elimination of H₂O₂ in RBCs include catalase, glutathione peroxidase (GPx) 1, and peroxiredoxins (Prxs) (17, 20, 21, 23, 24, 35).

GPx, which contains a selenocysteine (Sec) at its active site, catalyzes the reduction of hydroperoxides by glutathione

(GSH) (13). There are at least four types of GPx in mammalian cells, but GPx1 is the only type present in RBCs (24). Mammalian cells express six different Prx enzymes (11, 33), with Prx II being especially abundant in RBCs (22–24). Proteomic analysis has revealed that RBCs also contain small amounts of Prx I and Prx VI (27). All Prx enzymes contain a conserved cysteine residue (designated the peroxidatic cysteine, C_P) that corresponds to Cys-51 of Prx II (33). Four types of Prx (Prx I to Prx IV) contain an additional conserved Cys residue (the resolving cysteine, C_R) that corresponds to Cys-172 in Prx II. The Prx enzymes that contain two conserved cysteine residues are thus designated 2-Cys Prxs, whereas Prx VI is referred to as 1-Cys Prx because it contains only the C_P. In 2-Cys Prx enzymes, which are homodimers, C_P–SH of one subunit is selectively oxidized by peroxides to C_P–SOH, which then reacts with C_R–SH of the other subunit to produce an intermolecular disulfide bond (33). Reduction of the disulfide intermediate is mediated by thioredoxin (Trx) (10). Despite the fact that cysteine is much less sensitive to oxidation by peroxides than is selenocysteine, the bimolecular rate constant for C_P of Prx II was estimated to be $1.3 \times 10^7 \text{ M}^{-1} \text{ s}^{-1}$ (31), which is approaching that for GPx.

¹Division of Life and Pharmaceutical Sciences, Ewha Womans University, Seoul, Korea.

²School of Life Sciences and Biotechnology, Korea University, Seoul, Korea.

GPx is susceptible to inactivation by its own substrates. Exposure of purified GPx1 to various hydroperoxides gradually results in its irreversible inactivation (7, 32). The mechanism of inactivation of GPx by peroxide has remained unknown. Prx enzymes are also inactivated during catalysis. The C_P-SOH intermediate generated during catalysis occasionally undergoes further oxidation to sulfinic acid (C_P-SO₂H), leading to inactivation of peroxidase function (48). This hyperoxidation occurs only when Prx is engaged in the catalytic cycle. Reactivation of 2-Cys Prx enzymes is achieved by reduction of the C_P-SO₂H moiety in a reaction that requires ATP hydrolysis and is catalyzed by sulfiredoxin (Srx), with reducing equivalents such as GSH and Trx (5, 19, 46). Hyperoxidation to sulfinic acid is not restricted to Prx enzymes. Critical cysteine residues of many other proteins including glyceraldehyde-3-phosphate dehydrogenase (GAPDH) also undergo this modification. In contrast, reduction by Srx is highly selective. Among the Prx isoforms, only the sulfinic forms of the 2-Cys Prx subgroup (Prx I to Prx IV), not those of Prx V or Prx VI, are reduced by Srx (47). Moreover, Srx does not act on the sulfinic form of GAPDH (47). This specificity is due to the fact that Srx physically associates with the 2-Cys Prxs but not with other sulfinic proteins.

Among the antioxidant enzymes in RBCs, the activity of glutathione peroxidase 1 (GPx1) was shown to be strongly influenced by lifestyle and environmental factors such as use of dietary supplements and smoking habit and proposed as a strong predictor of cardiovascular risk, which is associated with oxidative stress (1, 6, 38). However, the mechanism underlying the influence of oxidative stress on GPx1 activity in RBCs has remained obscure. The average lifespan of human RBCs is 120 days. Given the limited capacity of RBCs to replace damaged proteins by *de novo* synthesis, inactivation of antioxidant enzymes would be expected to perturb the balance between oxidant production and elimination and thereby to accelerate the accumulation of ROS. We now show that oxidative stress induces an inactivation of GPx1 in RBCs and the inactivation is associated with the irreversible conversion of the Sec residue to dehydroalanine (DHA). We developed a convenient blot method for the detection of DHA-containing proteins, with the use of which we found that the amount of inactivated GPx1 is greater in RBCs of higher density. In contrast, immunoblot analysis revealed that the sulfinic form of Prxs was detected only when the H₂O₂ flux was increased above the basal level attributable to Hb autooxidation. These observations offer insight into the relative roles of catalase, GPx1, and Prxs in the elimination of H₂O₂ in RBCs.

Materials and Methods

Materials

N-(biotinoyl)-*N*-9'-(iodoacetyl)ethylenediamine (BIAM) was obtained from Molecular Probes (Carlsbad, CA). Horseradish peroxidase (HRP)-conjugated secondary antibodies, EZ-linked *N*-hydroxysuccinimide biotin, protein G-Sepharose beads, and HRP-conjugated streptavidin were from Pierce (Rockford, IL). Enhanced chemiluminescence (ECL) reagents, Prx I, Prx II, Prx VI, catalase, yeast glutathione reductase, a mouse monoclonal antibody to GPx1, as well as rabbit polyclonal antibodies to Prx I, to Prx II, to the sulfinic forms of 2-Cys Prxs, to Prx VI, to the sulfinic forms of Prx VI, to Srx, to

GAPDH, to the sulfinic forms of GAPDH, or to catalase were obtained from Young-In Frontier (Seoul, Korea). Cystamine-2HCl was from Sigma-Aldrich (St. Louis, MO).

Measurement of the selenol content of GPx1 after labeling with BIAM

Human RBCs were lysed by ultrasonic treatment in a solution containing 50 mM potassium phosphate (pH 6.5), 1 mM EDTA, 0.5% Triton X-100, 1% SDS, aprotinin (1 mg/ml), leupeptin (1 mg/ml), 1 μ M phenylmethylsulfonyl fluoride, and 10 mM BIAM; the solution was rendered free of O₂ by bubbling with N₂ gas. The lysates (or GPx1 purified from human RBCs) were then incubated for 30 min at room temperature, after which the labeling reaction was terminated by the addition of β -mercaptoethanol to a final concentration of 20 mM and the reaction mixture was centrifuged at 10,000 *g* for 10 min at 4°C. The resulting supernatant was diluted two-fold with PBS, subjected to immunoprecipitated as described below.

Immunoprecipitation and immunoblot analysis of GPx1

RBC lysates or reaction mixtures were incubated at 4°C first overnight with antibodies to GPx1 and then for 2 h in the additional presence of protein G-Sepharose beads. The beads were then separated by centrifugation and washed three times with ice-cold PBS, and the bead-bound proteins were fractionated by SDS-PAGE on a 14% gel and transferred to a nitrocellulose membrane for immunoblot analysis with antibodies to GPx1. Immune complexes were detected with HRP-conjugated secondary antibodies and ECL reagents.

Identification of DHA in GPx1 by MS/MS sequencing

GPx1 (30 μ g) purified from human RBCs was incubated with or without 1 mM H₂O₂ at 37°C for 1 h and then subjected to digestion with 0.6 μ g of bovine trypsin at 37°C for 15 h. The resulting peptides were fractionated by HPLC on a C₁₈ column with a linear gradient of 0 to 100% acetonitrile in 0.1% trifluoroacetic acid and at a flow rate of 1 ml/min. All fractions were collected and analyzed by MALDI-TOF mass spectrometry (MS) with a Voyager ion mirror reflector mass spectrometer (ABI, Foster City, CA). Mass spectra were interpreted with the use of the MS-Fit program (<http://prospector.ucsf.edu/prospector/mshome.html>). For peptide sequencing, the peptides were subjected to LC-ESI-Q-TOF tandem MS (Micromass, UK). The acquired spectra were processed and used to identify the peptide sequence with the use of MassLynx 4.0 software (Waters Co., Milford, MA).

Preparation of biotin-conjugated cysteamine

Cystamine 2HCl (150 μ l of a 50 mM solution in 0.1 M NaHCO₃) was incubated for 1 h at 25°C with 50 μ l of 50 mM EZ-linked *N*-hydroxysuccinimide biotin in DMF with vigorous shaking. The reaction was stopped by the addition of 50 μ l of 90 mM dithiothreitol, and the reaction mixture was then incubated for an additional 1 h with shaking before fractionation by HPLC on a C₁₈ column (4.6 by 25 cm; Vydac, W.R. Grace & Co., Deerfield, IL) with a linear gradient of 0 to 100% acetonitrile and at a flow rate of 1 ml/min. Fractions corresponding to the peak of biotin-conjugated cysteamine at 20.5 min were pooled and dried.

Detection of DHA-containing GPx1 after reaction with biotin-conjugated cysteamine

GPx1 was immunoprecipitated from RBC lysates with antibodies to GPx1, and the precipitates (or GPx1 purified from human RBCs) were subjected to alkylation with 10 mM iodoacetamide in the presence 1% SDS for 30 min at room temperature. Proteins were precipitated with trichloroacetic acid, dissolved in 0.1 M NaHCO₃ (pH 10.0) containing 1% SDS and 5 mM biotin-conjugated cysteamine, and incubated at 37°C for 18 h. Biotinylated proteins were then detected by SDS-PAGE and blot analysis with HRP-conjugated streptavidin as described above.

Assay of GPx1 activity

Human RBC lysate (40 µg of protein) was incubated for 15 h at 4°C in the wells of a 96-well plate coated with antibodies to GPx1. After washing the plate twice with a solution containing 20 mM Tris-HCl (pH 7.5), 500 mM NaCl, and 0.3% Tween-20, the reaction was performed in 200 µl of a solution containing 0.5 mM EDTA, 200 µM NADPH, 0.2 U of yeast glutathione reductase, 1 mM GSH, 1 mM *t*-butyl hydroperoxide, and 100 mM Tris-HCl (pH 7.0). The reaction was initiated by the addition of *t*-butyl hydroperoxide, and NADPH oxidation was monitored for 30 min at 30°C by measurement of the decrease in absorbance at 340 nm. The initial rate of the reaction was determined from the linear portion of the time course.

Purification of GPx1 from RBCs

GPx1 was purified from 4 l of human RBCs by a modified version of a previously described method (2). RBCs lysates were prepared, proteins were precipitated from the lysates by the addition of solid (NH₄)₂SO₄, and the precipitated proteins were dialyzed as described (2). The dialysate was subjected to sequential chromatographies on a column of CM-Sepharose (120 by 45 cm), a column of DEAE-Sepharose column (50 by 60 cm), a phenyl-5PW HPLC column (21.5 by 15 cm; toso-Hass), and a Superdex-200 HPLC column (10 by 30 cm). Column fractions were assayed by immunoblot analysis with antibodies to GPx1.

Purification of Sec49 → Cys GPx1 mutant from *Escherichia coli*

Human GPx1 mutant in which Sec⁴⁹ was replaced by cysteine residue were generated by standard PCR-mediated site-directed mutagenesis using GPx1 cDNA obtained from HeLa cells as the template and complementary primers containing a TGC that converts the codon (TGA) for Sec to one for Cys. The final mutated PCR products were ligated into the the NdeI and EcoRI sites of pET17b vector to generate pET 17b- GPx1-U49C. *Escherichia coli* BL21(DE3) competent cells (Novagen, Darmstadt, Germany) were transformed with pET17b-GPx1-U49C; cultured at 37°C for 5 h in 20 ml of LB medium with ampicillin (100 µg/ml); and then transferred to 2 liters of fresh LB medium, incubated at 37°C. When the absorbance of the culture at 600 nm reached 0.5, expression was induced by incubation of the cells for 3 h with 0.5 mM isopropyl-β-D-thiogalactopyranoside. The cells were harvested by centrifugation, and stored at -70°C until used. The Sec49 → Cys mutant was purified according to a method similar to that described for the purification of GPx1 from RBC.

Results

Effects of RBC aging on the catalytic activity and selenol content of GPx1 in RBCs

It is generally believed that the density of RBCs increases with RBC aging. We therefore fractionated human RBCs from healthy adult donors by centrifugation on a discontinuous density gradient of Percoll to obtain cells of four different mean densities (37). The activity of G6PDH, a marker of RBC aging (3, 29), decreased gradually with increasing RBC density (Fig. 1A). The activity of GPx1 also decreased with increasing RBC density, with the amount of GPx1 as determined by immunoblot analysis remaining constant (Fig. 1B). To determine whether the reduced GPx1 activity in the RBCs of higher density is accompanied by loss of selenol, we subjected RBC lysates to alkylation at pH 6.5 with BIAM. GPx1 was then immunoprecipitated and subjected to blot analysis with HRP-conjugated streptavidin (Fig. 1C). Although human GPx1 contains five Cys residues in addition to the active site Sec, selenol is selectively alkylated at pH 6.5 because it exists in the ionized form (-Se⁻), whereas thiols are in the protonated form (-SH) at this pH. The band intensity for BIAM-labeled GPx1 decreased with increasing RBC density, suggesting that a substantial proportion of GPx1 molecules in aged RBCs do not contain selenol. To provide concrete evidence that the selenol is the site of alkylation by BIAM, we prepared a mutant GPx1, in which Sec 49 was changed to Cys, and carried out the BIAM labeling experiment. Wild-type GPx1 was intensively labeled with BIAM, whereas no labeling was apparent with the mutant (Fig. 1D). In addition, H₂O₂ treatment decreased the labeling intensity of wild-type GPx1. These results indicate that Sec 49 is the only site of modification by BIAM and that oxidation of the selenol prevents BIAM labeling.

Conversion of Sec to DHA in GPx1 treated with H₂O₂

Tryptic peptides prepared from selenoproteins have previously been observed to have lost Sec residues as a result of their conversion to DHA during protein purification or digestion (25, 30). To determine whether GPx1 might lose selenium under oxidative stress, we incubated human GPx1 with 1 mM H₂O₂ for 1 h at 37°C. Such treatment resulted in ~40% loss of peroxidase activity (Fig. 2B). Samples of GPx1 that had been incubated in the absence or presence of H₂O₂ were digested with trypsin, and the resulting peptides were fractionated by HPLC on a C₁₈ column. Peptides were eluted between 20 and 60 min under the conditions described in Materials and Methods (not shown). Although the elution profiles of the two samples were similar, the pattern of peaks eluting between 39 and 40 min differed (Fig. 2C); treatment of GPx1 with H₂O₂ resulted in a decrease in the size of peak 1 (39.2 min) and the appearance of a new peak (peak 2) at 39.6 min. Peaks 1 and 2 were analyzed by LC-ESI-Q-TOF MS/MS. A selenium isotope distribution of 0.89% ⁷⁴Se, 9.37% ⁷⁶Se, 7.63% ⁷⁷Se, 23.77% ⁷⁸Se, 49.61% ⁸⁰Se, and 8.73% ⁸²Se rendered the Sec-containing peptide readily distinguishable from other peptides. Expanded spectra of peak 1 revealed an isotopic distribution typical of Se-containing peptides with a principal *m/z* peak at [M + 2H]²⁺ = 867.9 (Fig. 2D). The monoisotopic mass of 1733.8 Da calculated from this value corresponds to residues 39 TO 54 (VLLIENVASLUGTTVR,

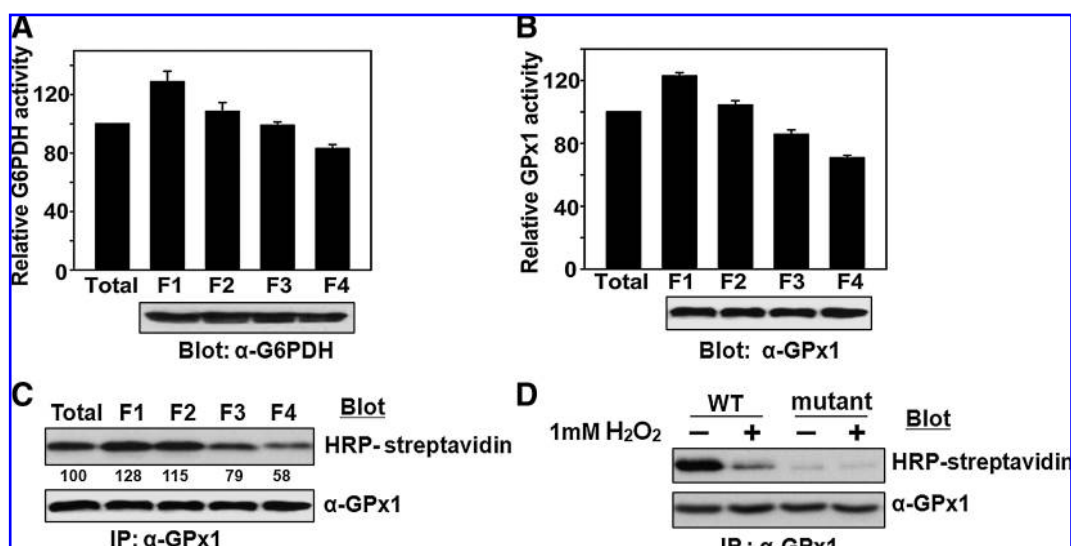


FIG. 1. Effect of aging on the catalytic activity and selenol content of GPx1 in RBCs. (A–C) Fresh RBCs obtained from a healthy human adult were separated on the basis of their density by centrifugation at 4,000 *g* for 15 min at 4°C on a discontinuous density gradient consisting of 85, 80, 76, 72, 69, and 66% Percoll (from the bottom up), as described previously (8). Among the six discrete bands obtained, the two minor bands at the top and bottom were discarded and the four middle bands (F1 to F4 for the least dense to the most dense, respectively) were used. The activity of G6PDH (A) in each fraction were measured according to the procedure described previously (29), and the activity of GPx1 (B) were measured, and their activities were normalized by the corresponding value for RBCs before fractionation. The fractions were also assayed for the selenol content of GPx1 (C); RBC lysates were subjected to alkylation with BIAM, GPx1 was immunoprecipitated (IP) from the lysates with antibodies to GPx1, and BIAM-labeled GPx1 in the precipitates was detected by blot analysis with HRP-conjugated streptavidin to measure selenol content (SeH). The band intensities are the average of three independent experiments. The presence of equal amounts of protein among assay mixtures was confirmed by immunoblot analysis with antibodies to G6PDH (A) or to GPx1 (B, C). Activity data in A and B are means \pm SD of triplicates from a representative experiment. (D) Wild-type (WT) and the Sec49 \rightarrow Cys mutant (mutant) GPx1 (10 μ g) were incubated in the absence or presence of 1 mM H₂O₂ for 1 h at 37°C and precipitated with trichloroacetic acid. The precipitated proteins were subjected to BIAM labeling, followed by HRP-conjugated streptavidin blot analysis as described in C.

where U denotes Sec) of GPx1 (theoretical mass = 1733.8 Da). Expanded ion signals of peak 2 yielded the usual isotopic distribution attributable to ¹³C (Fig. 2D), in contrast to the unusual distribution for the ions of peak 1. The principal *m/z* peak at $[M + 2H]^+ = 827.4$ corresponds to a molecular mass of 1652.8 Da (theoretical mass of 1652.9 Da). The observed difference of 81.0 Da between the molecular masses derived from the principal ions of peaks 1 and 2 is consistent with the loss of H₂Se (81.0 Da) and the concomitant generation of DHA in H₂O₂-treated GPx1. The sequence of the peptide corresponding to the principal ion of peak 2 and resulting from the conversion of Sec to DHA was confirmed by MS/MS analysis (Fig. 2E). The amino acid sequence determined from the *y* ion series was VLLIENVASLXGTTVR, which is identical to that inferred for the peptide corresponding to the principal ion of peak 1 with the exception that Sec at position 49 is replaced by an unknown residue X. The mass difference of 69.0 Da between *y*5 and *y*6 ions suggests that this unknown residue is DHA. Together, these results thus indicated that Sec is converted to DHA during exposure of GPx1 to H₂O₂.

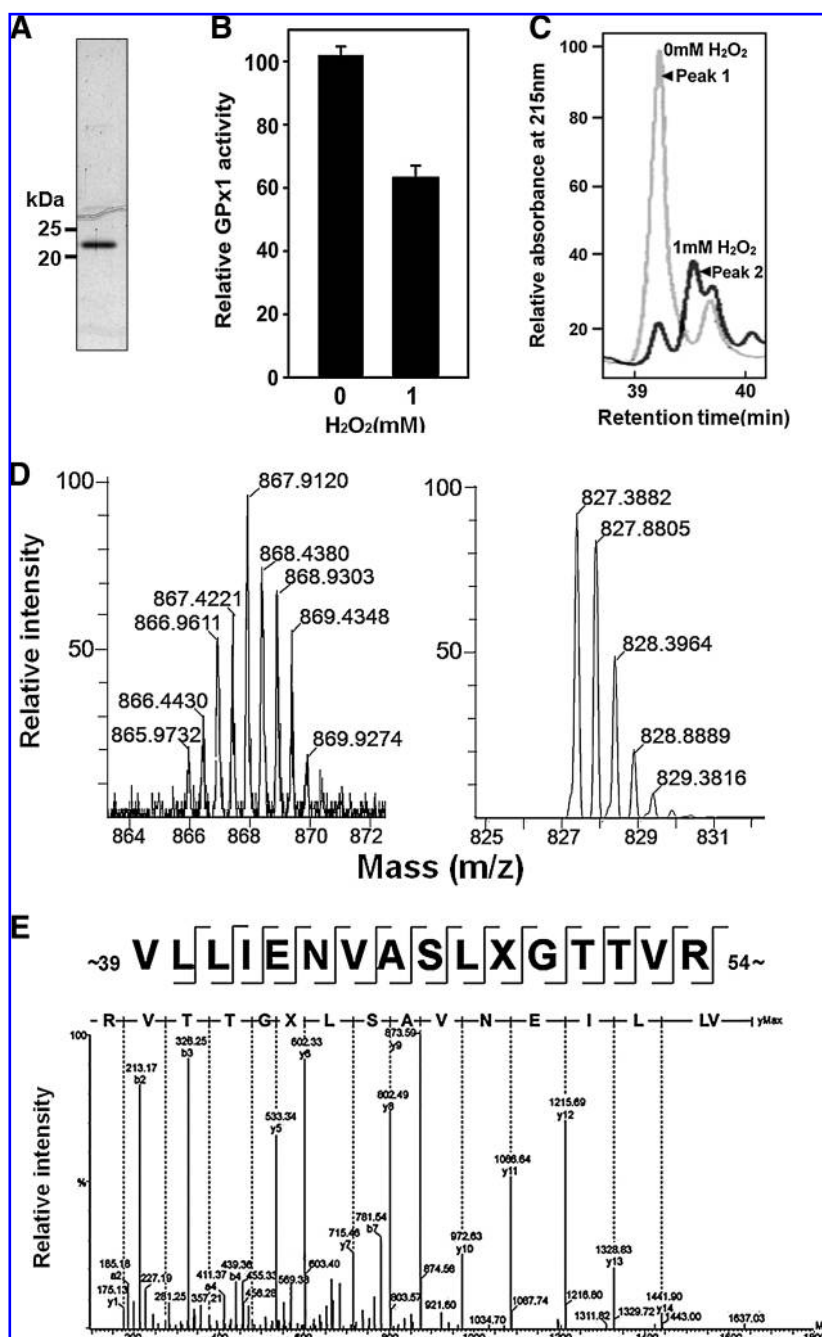
Detection of DHA-containing GPx1 in aged RBCs with the use of biotin-conjugated cysteamine

In order to detect DHA-containing GPx1 in cell lysates, we developed a method for specific labeling of DHA-containing

proteins with biotin-conjugated cysteamine. This method, which relies on the well-established Michael addition of cysteamine to the DHA moiety (Fig. 3A), involves the immunoprecipitation of GPx1 from cell extracts and the alkylation of Cys-SH and intact Sec-SeH in the precipitated proteins with iodoacetamide. The precipitated proteins are then incubated with biotin-conjugated cysteamine to biotinylate DHA-containing GPx1, which is detected by SDS-PAGE followed by blot analysis with HRP-conjugated streptavidin.

We applied this method to determine whether the conversion of Sec to DHA in GPx1 occurs with aging of RBCs. Indeed, the blot intensity of the band recognized by HRP-conjugated streptavidin increased gradually with increasing RBC density, which is correlated with increasing RBC age (Fig. 3B), indicating that the Sec residue of GPx1 is converted to DHA in a time-dependent manner during exposure to the mild oxidative stress resulting from heme autooxidation. The DHA detection method was validated using purified GPx1 (Fig. 3C). When purified enzyme was exposed for 1 h to various amounts (0, 0.2, 0.5, or 1 mM) of H₂O₂, the enzyme activity and the selenol content measured by BIAM labeling decreased in parallel in association with the increased H₂O₂ concentration. On the other hand, the DHA content measured by biotin-conjugated cysteamine increased with increased H₂O₂ concentration.

FIG. 2. Identification of DHA in H₂O₂-treated GPx1 by MS. (A) Purified human GPx1 was subjected to SDS-PAGE analysis on a 14% gel. Size markers are indicated. (B) Purified GPx1 (30 μ g) was incubated in the absence or presence of 1 mM H₂O₂ for 1 h at 37°C and then assayed for GPx1 activity. Data are means \pm SD of triplicates from a representative experiment. (C) GPx1 incubated with (dark gray line) or without (light gray line) H₂O₂ as in B was subjected to tryptic digestion, and the resulting peptides were fractionated by HPLC on a C₁₈ column. Peaks eluting between 39 and 40 min are shown. (D) Expanded LC-ESI-Q-TOF tandem MS spectra for peptides corresponding to peak 1 (left panel) or peak 2 (right panel) from C. The isotopic distribution was normalized relative to the largest peak. (E) Tandem MS spectrum obtained from fragmentation of the doubly charged ion with an m/z of 827.4 from peak 2 in D. The y ion series defined the indicated amino acid sequence. The mass difference of 69.0 Da between the y5 and y6 ions defined residue X as DHA.



Effects of aging on production of the sulfinic forms of Prxs and GAPDH

We also investigated whether the inactivated sulfinic forms of Prx enzymes accumulate in aged RBCs. Sulfinic Prxs can be detected by immunoblot analysis with antibodies that recognize a specific sequence surrounding the C_P-SO₂H (47). Because the active site sequence (DFTFVCPT_{EL}) is the same for 2-Cys Prxs (Prx I to IV) and because the sizes of Prx I and Prx II are identical, the sulfinic forms of Prx I and Prx II cannot be differentiated by immunoblot analysis. Sulfinic Prx VI, however, can be distinguished because its active site sequence (DFTPVCT_{TEL}) differs from that for 2-Cys Prxs and because specific antibodies that recognize the sulfinic form are avail-

able. Immunoblot analysis with the antibodies to sulfinic Prxs revealed that neither the sulfinic form of Prx I or Prx II nor that of Prx VI is detected in RBCs of higher density, indicating sulfinic Prxs do not accumulate during the aging process (Fig. 4A). In contrast, the amount of the sulfinic form of GAPDH increased markedly during aging (Fig. 4A). Sulfenylation of proteins induces an acidic shift in their position on two-dimensional gels. Analysis of the age-related RBC fractions by 2D-PAGE did not reveal an acidic shift of Prx II (Fig. 4B), consistent with the results of immunoblot analysis with the antibodies to sulfinic 2-Cys Prxs. Given that Prx II is abundant in RBCs, the conversion of even a small proportion of Prx II molecules to the sulfinic form would be expected to be readily detected by both types of analysis. Srx is expressed in RBCs

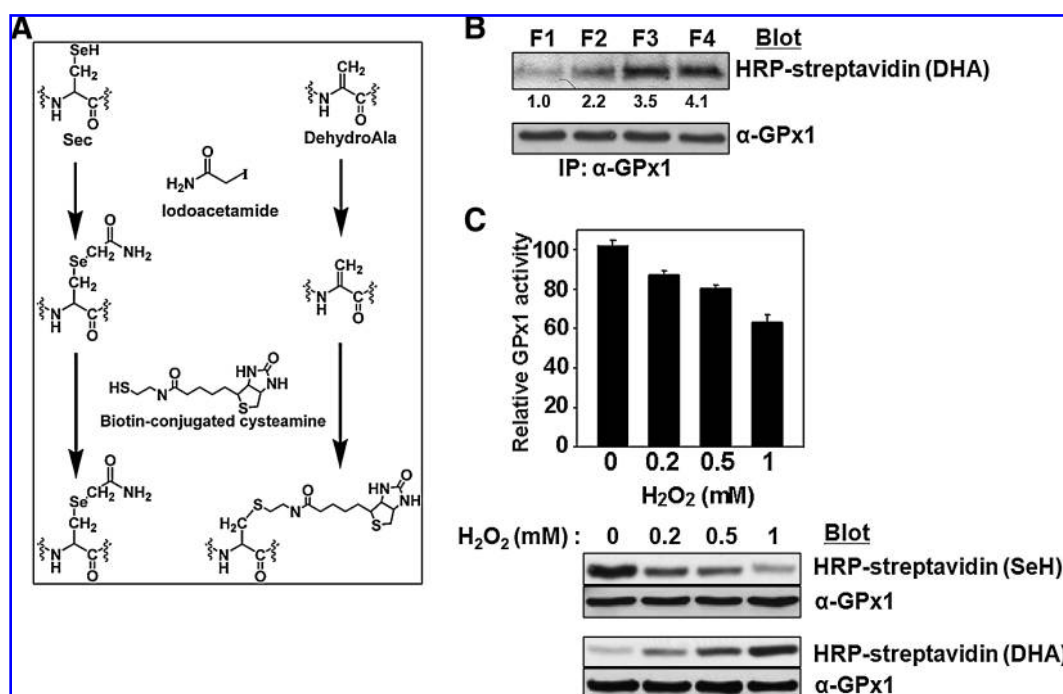


FIG. 3. Effect of aging and H₂O₂ treatment on the DHA content of GPx1 as revealed by blot analysis after reaction with biotin-conjugated cysteamine. (A) Chemical reactions underlying the biotinylation of GPx1 containing DHA. After alkylation of free SH and SeH groups by iodoacetamide, DHA residues are biotinylated with biotin-conjugated cysteamine. (B) Fresh RBCs were separated into four fractions (F1, F2, F3, and F4) on the basis of their density (age) as in Fig. 1, and GPx1 was immunoprecipitated from the lysate of each fraction and analyzed for DHA content by sequential reaction with iodoacetamide and biotin-conjugated cysteamine as outlined in A. The band intensities are average of three independent experiments. (C) After incubation of purified GPx1 (10 μg) at 37°C for 1 h with various amounts (0, 0.2, 0.5, or 1 mM) of H₂O₂, GPx activity, selenol content (SeH), and DHA-content were measured as described above.

and its abundance remained unchanged during aging (Fig. 4A).

Effects on antioxidant enzymes in RBCs of extracellular H₂O₂ produced by GO

H₂O₂ passes through the plasma membrane of RBCs, and antioxidant enzymes in RBCs eliminate ROS that originate from the external environment and thereby protect other cells from oxidative injury induced by phagocytic cells or toxins (44). To examine the effects of extracellular H₂O₂ on RBCs, we added various amounts of glucose oxidase (GO) to these cells (50% hematocrit) suspended in DMEM containing a high concentration of glucose. GO catalyzes the oxidation glucose with concomitant production of H₂O₂. Incubation of RBCs with GO at 37°C for 3 h resulted in concentration-dependent decreases in the activity (Fig. 5A) and selenol content (Fig. 5B) of GPx1 as well as an increase in the DHA content of GPx1 (Fig. 5C). Although the sulfinic forms of Prx II and Prx VI were not detected in aged RBCs (Fig. 4), their accumulation was apparent in cells incubated in the presence of GO at 0.1 mU/ml and increased further at higher concentrations of GO (Fig. 5D). This accumulation of sulfinic Prx II was confirmed by 2D-PAGE, with 0, 10, 25, and 70% of Prx II being estimated to be oxidized to the sulfinic form in the presence of GO at 0, 0.1, 0.5, and 1.0 mU/ml, respectively (Fig. 5E). The amount of Srx in RBCs was not affected by the presence of GO (Fig. 5D). The sulfinic form of GAPDH was detected in RBCs

even in the absence of GO (Fig. 4A), but its abundance increased in the presence of GO (Fig. 5D). The amount of H₂O₂ produced by GO under our experimental conditions was estimated. In the absence of RBCs, GO at 1 mU/ml generated H₂O₂ at a rate of ~45 μM/min (Fig. 5F). However, accumulation of H₂O₂ was not detected when the same amount of GO was added to the suspension of RBCs (Fig. 5F); indeed, no accumulation of H₂O₂ was detected even at a GO concentration of 50 mU/ml, which could produce H₂O₂ at a rate of ~2.25 mM/min in the absence of RBCs (not shown). These observations indicate that human blood is able to metabolize H₂O₂ efficiently by catalase in RBCs. Nevertheless, the entry of H₂O₂ into RBCs induces oxidative damage to many proteins including G6PDH and GAPDH. In addition, loss of the Sec residue of GPx1 is accelerated even at a low rate of H₂O₂ entry (4.5 μM/min, as generated by GO at 0.1 mU/ml). Furthermore, the hyperoxidation of Prx II and Prx VI, which was not observed during normal aging of RBCs, becomes apparent at the rate of H₂O₂ entry.

Effects of N-phenylhydroxylamine on antioxidant enzymes in RBCs

A variety of drugs including sulfonamides and industrial chemicals such as aniline induce hemolytic anemia (4, 15, 40). These arylamine compounds are metabolized in the liver, and the resulting N-hydroxyarylamines react with oxyHb to produce superoxide anion.

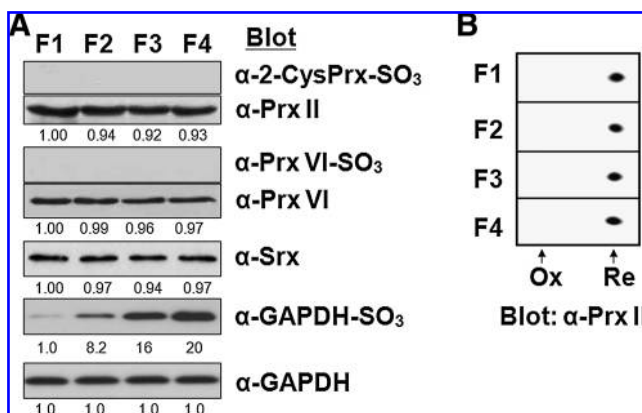


FIG. 4. Effects of aging on generation of the sulfinic forms of Prx enzymes or GAPDH. (A) Fresh RBCs were separated into four fractions (F1, F2, F3, and F4) on the basis of their density (age), and lysates of each fraction were subjected to immunoblot analysis with antibodies specific for the sulfinic form of 2-Cys Prxs, Prx VI, or GAPDH. Equal loading of proteins was confirmed by immunoblot analysis with antibodies to Prx II, to Prx VI, and to GAPDH, respectively. Immunoblot analysis was also performed with antibodies to Srx. The band intensities are average of two independent experiments. (B) Lysates of the age-related fractions of RBCs were also subjected to two-dimensional PAGE on a 13-cm Immobiline DryStrips (Amersham; pH 4 to 7, linear) and probed by immunoblot analysis with antibodies to Prx II(20). The positions of hyperoxidized (Ox) and reduced (Re) forms of Prx II are indicated.

To examine the effects of such extra oxidative stress produced internally by an environmental chemical, we incubated a 50% hematocrit of RBCs with 200 μ M *N*-phenylhydroxylamine for various times. The activity (Fig. 6A) and selenol content (Fig. 6B) of GPx1 decreased with time whereas the DHA content of GPx1 increased (Fig. 6C) on exposure of RBCs to *N*-phenylhydroxylamine. ROS produced by *N*-phenylhydroxylamine also induced hyperoxidation of Prx II, Prx VI, and GAPDH (Fig. 6D).

Effect of catalase inhibition on Prx II hyperoxidation

Catalase is inhibited specifically by 3-amino-1,2,4-triazole (3-AT) (26). This inhibitory action is only apparent in the presence of H₂O₂ because it is exerted on compound I. Catalase is inhibited nonspecifically by azide. Sodium azide (10 mM) or 3-AT (50 mM) was added to a 50% hematocrit of RBCs in DMEM containing high glucose before exposure of the cells to various concentrations of GO. After incubation of the RBC suspension for various times, cell lysates were subjected to immunoblot analysis with antibodies to the sulfinic form of 2-Cys Prxs (Fig. 7A). RBC lysates analyzed in Fig. 5E were included in the immunoblot analysis as hyperoxidation standards; in standards 1 and 2, ~10, and ~25%, respectively, of Prx II was hyperoxidized as the result of incubation with GO at 0.1 and 0.5 mU/ml, respectively, for 3 h. In the absence of GO, inhibition of catalase did not induce Prx II hyperoxidation (Fig. 7A). In the presence of GO at 0.1 or 0.5 mU/ml, Prx II was slowly hyperoxidized and this effect was accelerated by a factor of 5 to 10 when catalase was inhibited (Fig. 7A). We also evaluated the effect of catalase in-

hibition on GPx1-DHA formation (Fig. 7B). Although the effect was not as pronounced as that on Prx II hyperoxidation, the absence of catalase activity clearly increased GPx1-DHA formation. These results suggest that the absence of catalase activity is not enough of a burden to the Prx II and GPx1 systems to result in hyperoxidation of Prx II or irreversible oxidation of GPx1 unless H₂O₂ enters RBCs from the external environment.

Discussion

We have shown that the Sec residue of GPx1 is converted to DHA during aging of RBCs *in vivo*. Our observation that treatment of purified GPx1 with H₂O₂ induces the conversion of Sec to DHA suggests that an oxidative environment promotes the conversion of GPx-SeH to GPx-SeO₂H and subsequent loss of H₂SeO₂ *via* β -elimination. Treatment of GPx with H₂O₂ has been shown to generate GPx-SeO₂H (41). We developed a convenient method for estimation of the amount of DHA-GPx1 in cell homogenates. This blot-based method depends on specific addition of biotin-conjugated cysteamine to the DHA residue followed by detection of biotinylated protein based on its interaction with streptavidin. With the use of this method, we found that conversion of the Sec residue of GPx1 to DHA occurred during aging of RBCs *in vivo* as well as in RBCs exposed to H₂O₂ generated either externally by GO or internally as a result of *N*-phenylhydroxylamine-induced Hb autooxidation.

Selenocysteine is not the only source of DHA in cells. Cysteine residues of many proteins are present in the form of Cys-SO₂H in normal tissues (14) and some of them are converted to DHA (39). However, DHA is not frequently found in positions corresponding to Cys residues. This difference is likely attributable to the greater strength of the C-S bond (272 kJ/mol) compared with that of the C-Se bond (234 kJ/mol) (25). These multiple sources of DHA are consistent with our observation that direct blot analysis of crude RBC extracts yielded many positive bands (not shown). It was thus necessary to immunoprecipitate GPx1 before alkylation and labeling with biotin-conjugated cysteamine in order to measure DHA specifically in GPx1.

The concentration of Prx II was reported to be ~240 μ M (28). In contrast, Prx I and Prx VI are present at concentrations that are only ~1% of that of Prx II (data not shown). During the catalytic cycle of Prx II, the intermolecular C_P-C_R disulfide is reduced by Trx1, which has been suggested to be the limiting step in the process of H₂O₂ elimination in RBCs because the concentration of thioredoxin reductase 1 (TrxR1), the enzyme required for the reduction of oxidized Trx1, is low in RBCs (23). Nevertheless, Prx II molecules were found as monomers with the C_P residue in the thiol state in RBCs obtained from normal individuals (23), suggesting that the reducing capacity of the Trx system in RBCs is sufficient to maintain Prx II in its reduced form while confronting the basal level of H₂O₂ flux originating from Hb autooxidation. It appears, however, that the Trx system does not have much extra capacity to cope with a small increase in H₂O₂ flux, given that Prx II molecules were found in the disulfide-linked dimeric state in RBCs treated for 10 min with H₂O₂ at a concentration as low as 0.5 μ M (23).

Although Prx II is mainly responsible for dealing with the basal level of H₂O₂ flux originating from Hb autooxidation (20,

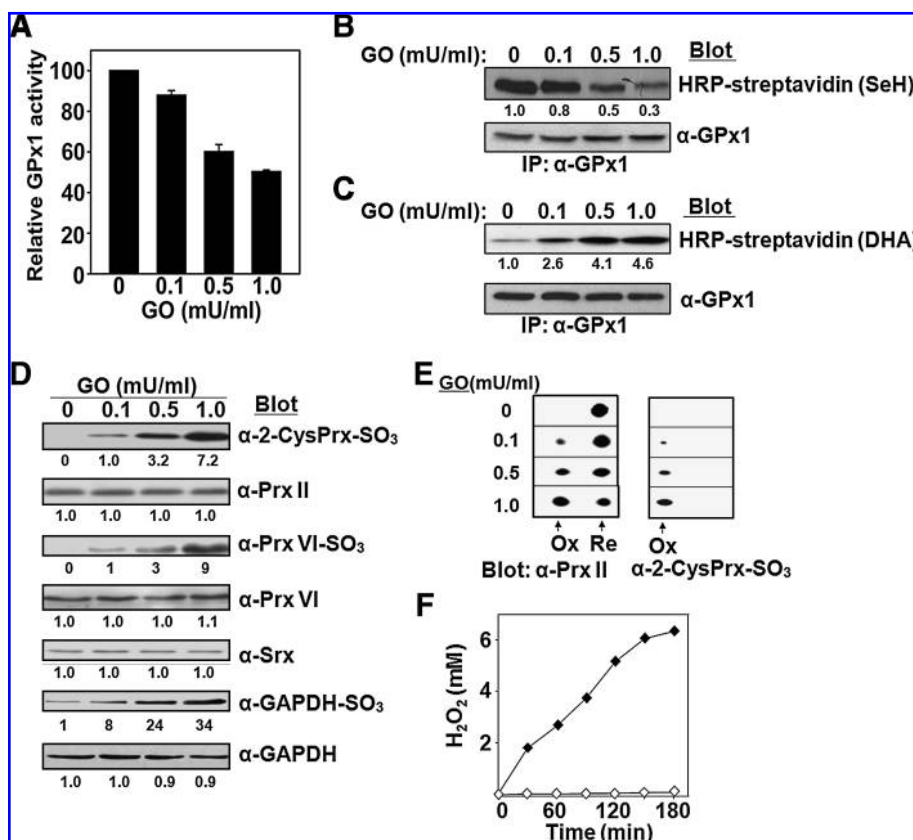


FIG. 5. Effects on antioxidant enzymes in RBCs of extracellular H₂O₂ produced by GO. (A–E) Various amounts (0, 0.1, 0.5, or 1 mU) of glucose oxidase (GO) were added to 1 ml of RBCs at a 50% hematocrit in DMEM containing a high concentration (4,500 mg/l) of glucose. After incubation for 3 h with gentle shaking at 37°C, the RBCs were lysed and subjected to the following analyses: (A) Measurement of GPx1 activity and its normalization by that of RBCs incubated in the absence of GO. Data are means \pm SD of triplicates from a representative experiment. (B, C) Determination of the selenol (SeH) and DHA contents, respectively, of GPx1. Equal loading of proteins was confirmed by immunoblot analysis with antibodies to GPx1. (D) Immunoblot analysis with antibodies specific for the sulfinic forms of 2-Cys Prxs, Prx VI, or GAPDH. Equal loading of proteins was confirmed by immunoblot analysis with antibodies to Prx II, to Prx VI, or to GAPDH, respectively. Immunoblot analysis was also performed with an-

tibodies to Srx. The band intensities shown in B–D are average of two independent experiments. (E) Two-dimensional PAGE followed by immunoblot analysis with antibodies to Prx II and to the sulfinic form of 2-Cys Prxs. The positions of hyperoxidized (Ox) and reduced (Re) forms of Prx II are indicated. (F) The H₂O₂ concentration generated by incubation of GO at 1 mU/ml in the absence (solid diamonds) or presence (open diamonds) of RBCs at a 50% hematocrit was measured on the basis of ferrous oxidation of xylenol orange (45).

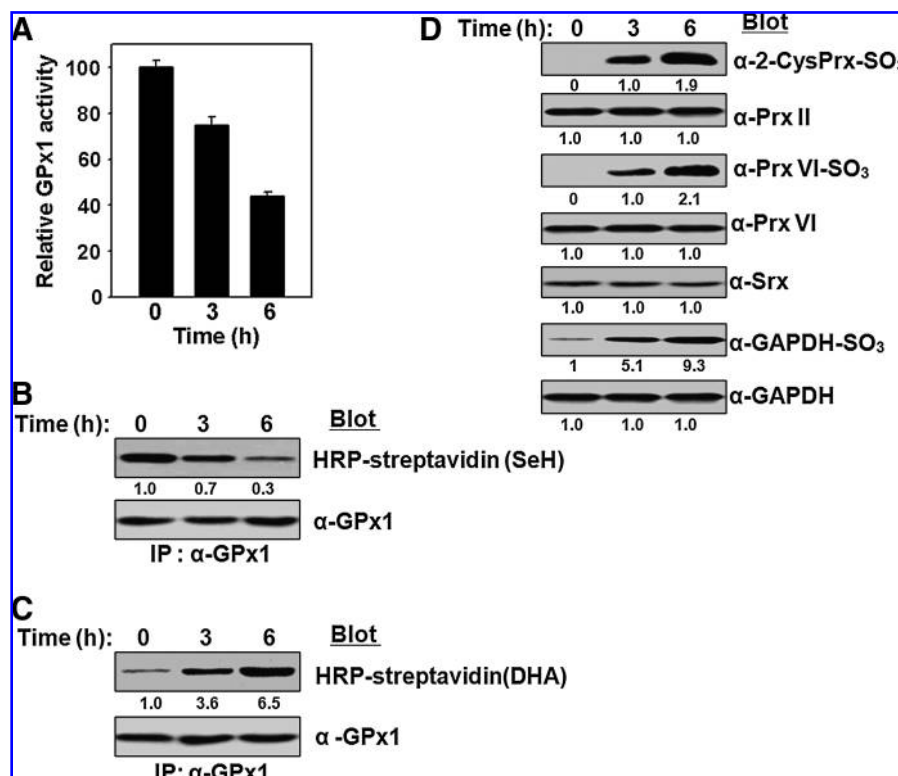
23), we did not detect sulfinic Prx II in aged RBCs. These findings are likely attributable to the fact that RBCs contain Srx at a sufficient concentration to counteract the hyperoxidation. If we assume that autooxidation occurs at a rate of 3% of total Hb a day in the 50% hematocrit suspension and that all superoxide anions produced from the autooxidation are dismutated to H₂O₂, the rate of H₂O₂ production in the suspension would be $\sim 0.1 \mu\text{M}/\text{min}$. When RBCs at a 50% hematocrit were incubated for 3 h with GO at 0.1 mU/ml, which generates H₂O₂ at a rate of $\sim 4.5 \mu\text{M}/\text{min}$, $\sim 10\%$ of Prx II was found to be hyperoxidized. The hyperoxidation rate is proportional to the rate at which Prx eliminates H₂O₂ (48). This result suggests that the additional flux of H₂O₂ at a rate of $\sim 4.5 \mu\text{M}/\text{min}$ increases the hyperoxidation of Prx II to a level that exceeds the capacity of Srx in RBCs. Inhibition of catalase by azide or 3-AT did not increase H₂O₂ flux enough to induce accumulation of hyperoxidized Prx II, suggesting that Srx might still be able to counteract the additional flux of H₂O₂ arising from the inactivation of catalase function. However, catalase inhibition accelerated Prx II hyperoxidation 5- to 10-fold in RBCs exposed to GO at 0.1 or 0.5 mU/ml, suggesting that catalase becomes important for removal of H₂O₂ if the flux of H₂O₂ is increased, such as a result of exposure of RBCs to external H₂O₂ or to a toxin that increases intracellular H₂O₂

production. GPx1-DHA formation was enhanced moderately when catalase was inhibited by azide or 3-AT.

Although ping-pong kinetics make it difficult to describe the enzymatic characteristics of Prx, GPx, and catalase by conventional V_{max} and K_m terms, various kinetic data suggest that Prx II is responsible for eliminating low concentrations of peroxides, whereas catalase scavenges H₂O₂ efficiently at high concentrations (20, 23, 31). This conclusion is also supported by *in vivo* evidence: Mice that lack Prx II develop hemolytic anemia (22), whereas RBC-related defects are not apparent in catalase-deficient mice (17).

Prx II, with a concentration of $\sim 240 \mu\text{M}$ ($\sim 100 \mu\text{M}$ in blood), is one of the most abundant proteins in RBCs. Prx II would thus be expected to be able to remove H₂O₂ rapidly if its level in blood increases up to $\sim 100 \mu\text{M}$. However, as suggested before (23), this removal would be attributable to one-time noncatalytic scavenging, given that all Prx II molecules would accumulate as the disulfide-linked dimer of the catalytic cycle as a result of the limited capacity of the Trx system in RBCs. Reduction of the dimeric Prx II might take as long as 20 min (23). Under these circumstances, elimination of additional H₂O₂ would depend on catalase action. Indeed, RBCs that lack catalase are highly sensitive to exogenous H₂O₂ (18), suggesting that catalase is essential for protection

FIG. 6. Effects of N-phenylhydroxylamine on antioxidant enzymes in RBCs. N-phenylhydroxylamine (200 μ M) was added to a 50% hematocrit of RBCs in DMEM containing a high glucose concentration (4500 mg/l). After incubation for various times (0, 3, or 6 h) with gentle shaking at 37°C, the RBCs were lysed and subjected to the following analyses: (A) Measurement of GPx1 activity and its normalization relative to that of cells incubated in the absence of N-phenylhydroxylamine (time 0). Data are means \pm SD of triplicates from a representative experiment. (B, C) Determination of the selenol (SeH) and DHA contents, respectively, of GPx1. Equal loading of proteins was confirmed by immunoblot analysis with antibodies to GPx1. (D) Immunoblot analysis with antibodies specific for the sulfinic forms of 2-Cys Prxs, Prx VI, or GAPDH. Equal loading of proteins was confirmed by immunoblot analysis with antibodies to Prx II, to Prx VI, and to GAPDH, respectively. Immunoblot analysis was also performed with antibodies to Srx. The band intensities shown in B–D are the average of two independent experiments.



against higher levels of H₂O₂. The antioxidant role of GPx in various types of cells including RBCs has been discussed for many years (9). Recently, GPx1 has been suggested to play a minor role in the elimination of H₂O₂ from RBCs, given that mice lacking GPx1 appear normal (16) and RBCs derived from these mice show a virtually normal defense against exogenous H₂O₂ so long as catalase function is intact (21). The primary physiological substrate of GPx1 has been proposed to be organic peroxides rather than H₂O₂ (21). Special care has to be taken, however, in extrapolating the results obtained with GPx 1 KO mice to physiology of human RBCs because the relative activities of antioxidant enzymes in RBCs are different in the two species (20).

Catalase, as a dismutase, does not require reducing equivalents to eliminate H₂O₂, whereas GPx1 and Prx II require the GSH and Trx systems, respectively, both of which derive reducing equivalents from NADPH. Glutathione reductase, TrxR, and G6PDH, which are critical for the production of GSH, reduced Trx, and NADPH, respectively, are all sensitive to inactivation by H₂O₂ (3, 12, 36). GPx1 and Prx II are thus expected to become less efficient when RBCs are exposed to high levels of oxidative stress for long periods because the recycling of GSH and Trx becomes rate limiting. Even under such stressful circumstances, catalase alone is able to remove H₂O₂ rapidly as a result of its high turnover rate. However, two problems arise. First, organic peroxides will accumulate because catalase cannot remove them. Second, the intracellular concentration of H₂O₂ will be much higher than that maintained in the presence of fully functional GPx1 and Prx II because catalase is not able to function effectively when

the H₂O₂ concentration falls. The steady-state level of H₂O₂ in mouse RBCs is estimated to be 0.05 nM (20). This extremely low level of H₂O₂, which is mainly attributable to the activity of Prx II, ensures protection of cell components from oxidative damage. The energy-consuming function of Prx II is thus needed in addition to the energy-independent catalase for RBC homeostasis.

GPx1 and Prx II are inactivated as the result of oxidative modification of Sec and Cys residues, respectively, at the active site. Our results now show that GPx1 inactivation is irreversible and does not require continuous turnover, whereas Prx II inactivation is reversible and progresses only when the enzyme goes through the catalytic cycle continuously (48). We found that the inactive DHA-GPx1 accumulates in RBCs with age even under the basal condition of H₂O₂ flux originating from Hb autooxidation. The inactive, sulfinic form of Prx II, however, does not accumulate under this condition. Our results indicate that the amount of sulfinic Prx II increases transiently when the flux of H₂O₂ increases temporarily above the basal level, but it might be removed slowly by the action of Srx. When exposed to such an increased H₂O₂ flux for long periods, however, the inactivated forms of both Prx II and GPx1 accumulate, as seen in RBCs exposed to GO, to N-phenylhydroxylamine, or to a catalase inhibitor in the presence of a low concentration of GO. Under these circumstances, catalase becomes the main player, and the concentrations of intracellular H₂O₂ and organic peroxides are expected to rise.

RBCs protect other tissues against oxidative damage by taking up and metabolizing peroxides (44). Given that the rate of DHA-GPx1 accumulation in RBCs depends on peroxide

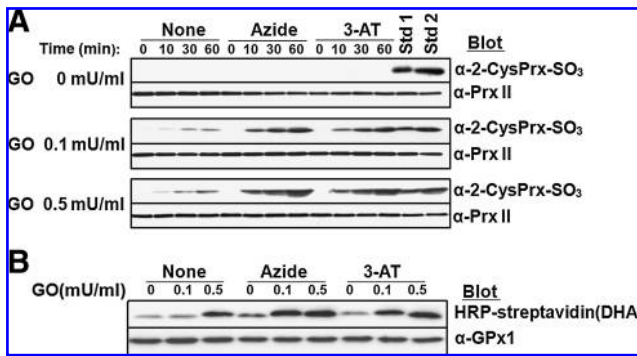


FIG. 7. Effect of catalase inhibition on Prx II hyperoxidation and GPx1-DHA formation. RBCs at a 50% hematocrit in DMEM containing high glucose (4500 mg/l) were incubated at 37°C first for 10 min in the absence or presence of 10 mM sodium azide or 50 mM 3-AT and then for the indicated times (0, 10, 30, and 60 min) in the additional presence of various concentrations (0, 0.1, or 0.5 mU/ml) of GO. (A) The cells were then lysed and subjected to immunoblot analysis with antibodies specific for the sulfinic form of 2-Cys Prxs. Equal loading of proteins was confirmed by immunoblot analysis with antibodies to Prx II. Lysates of RBCs that had been treated with GO at 0.1 mU/ml (Std 1) or 0.5 mU/ml (Std 2) for 3 h (Fig. 5E) were included in the immunoblot analysis as standards; in these standard samples, ~10 and ~25% of Prx II was hyperoxidized as judged on the basis of 2D-PAGE analysis. (B) RBCs that had been incubated for 60 min with various concentrations (0, 0.1, or 0.5 mU/ml) of GO in the absence or presence of 10 mM sodium azide or 50 mM 3-AT as in A were lysed, and the lysates were then subjected to the determination of DHA contents. Equal loading of proteins was confirmed by immunoblot analysis with antibodies to GPx1.

flux, the content of DHA-GPx1 in each RBC likely reflects total oxidative stress experienced by the cell during its lifetime. In addition to genetic polymorphisms, exposure to chemicals such as N-phenylhydroxylamine and sulfonamides, pathological conditions such as diabetes and local inflammation, and an insufficient intake of antioxidants are all expected to affect the rate of GPx1 inactivation. Our present data suggest that DHA-GPx1 in RBCs might be a suitable surrogate marker for evaluation of oxidative stress in the body.

Acknowledgments

This study was supported by Korean Science and Engineering Foundation grants (National Honor Scientist Program grant 2006-05106 and grant FPR0502-470 of the 21C Frontier Functional Proteomics Projects) to S.G.R.

Author Disclosure Statement

S.G.R. is a member of the advisory board of Young-In Frontier.

References

- Andersen HR, Nielsen JB, Nielsen F, and Grandjean P. Antioxidative enzyme activities in human erythrocytes. *Clin Chem* 43: 562–568, 1997.
- Awasthi YC, Beutler E, and Srivastava SK. Purification and properties of human erythrocyte glutathione peroxidase. *J Biol Chem* 250: 5144–5149, 1975.
- Bartosch, G. Aging of the erythrocyte. VII. On the possible causes of inactivation of red cell enzymes. *Mech Ageing Dev* 13: 379–385, 1980.
- Beutler, E. The hemolytic effect of primaquine and related compounds: A review. *Blood* 14: 103–139, 1959.
- Biteau B, Labarre J, and Toledano MB. ATP-dependent reduction of cysteine-sulfinic acid by *S. cerevisiae* sulphiredoxin. *Nature* 425: 980–984, 2003.
- Blankenberg S, Rupprecht HJ, Bickel C, Torzewski M, Hafner G, Tiet L, Smieja M, Cambien F, Meyer J, and Lackner KJ. Glutathione peroxidase 1 activity and cardiovascular events in patients with coronary artery disease. *N Engl J Med* 349: 1605–1613, 2003.
- Blum J and Fridovich I. Inactivation of glutathione peroxidase by superoxide radical. *Arch Biochem Biophys* 240: 500–508, 1985.
- Boyer C, Kahn A, Cottreau D, and Marie J. [Mechanism of decrease in erythrocyte enzyme activities during red cell aging in the newborn and the adult]. *Nouv Rev Fr Hematol Blood Cells* 18: 229–231, 1977.
- Brigelius-Flohe, R. Tissue-specific functions of individual glutathione peroxidases. *Free Radic Biol Med* 27: 951–965, 1999.
- Chae HZ, Chung SJ, and Rhee SG. Thioredoxin-dependent peroxide reductase from yeast. *J Biol Chem* 269: 27670–27678, 1994.
- Chae HZ, Robison K, Poole LB, Church G, Storz G, and Rhee SG. Cloning and sequencing of thiol-specific antioxidant from mammalian brain: alkyl hydroperoxide reductase and thiol-specific antioxidant define a large family of antioxidant enzymes. *Proc Natl Acad Sci USA* 91: 7017–7021, 1994.
- Dincer Y, Akcay T, Alademir Z, and Ilkova H. Effect of oxidative stress on glutathione pathway in red blood cells from patients with insulin-dependent diabetes mellitus. *Metabolism* 51: 1360–1362, 2002.
- Flohe L and Brigelius-Flohe R. Selenoproteins of the glutathione system. In: *Selenium. Its Molecular Biology and Role in Human Health*, edited by Hatfield, dl. Boston, Dordrecht, London: Kluwer Academic Publishers. 2001. pp. 161–172.
- Hamann M, Zhang T, Hendrich S, and Thomas JA. Quantitation of protein sulfinic and sulfonic acid, irreversibly oxidized protein cysteine sites in cellular proteins. *Methods Enzymol* 348: 146–156, 2002.
- Harrison JH, Jr. and Jollow DJ. Role of aniline metabolites in aniline-induced hemolytic anemia. *J Pharmacol Exp Ther* 238: 1045–1054, 1986.
- Ho YS, Magnenat JL, RBronson RT, Cao J, Gargano M, Sugawara M, and Funk CD. Mice deficient in cellular glutathione peroxidase develop normally and show no increased sensitivity to hyperoxia. *J Biol Chem* 272: 16644–16651, 1997.
- Ho YS, Xiong Y, Ma W, Spector A, and Ho DS. Mice lacking catalase develop normally but show differential sensitivity to oxidant tissue injury. *J Biol Chem* 279: 32804–32812, 2004.
- Jacob HS, Ingbar SH, and Jandl JH. Oxidative hemolysis and erythrocyte metabolism in hereditary acatalasia. *J Clin Invest* 44: 1187–1199, 1965.
- Jeong W, Park SJ, Chang TS, Lee DY, and Rhee SG. Molecular mechanism of the reduction of cysteine sulfinic acid of peroxiredoxin to cysteine by mammalian sulfiredoxin. *J Biol Chem* 281: 14400–14407, 2006.

20. Johnson RM, Goyette G Jr, Ravindranath Y, and Ho YS. Hemoglobin autooxidation and regulation of endogenous H₂O₂ levels in erythrocytes. *Free Radic Biol Med* 39: 1407–1417, 2005.
21. Johnson RM, Goyette G Jr, Ravindranath Y, and Ho YS. Red cells from glutathione peroxidase-1-deficient mice have nearly normal defenses against exogenous peroxides. *Blood* 96: 1985–1988, 2000.
22. Lee TH, Kim SU, Yu SL, Kim SH, Park DS, Moon HB, Dho SH, Kwon KS, Kwon HJ, Han YH, Jeong S, Kang SW, Shin HS, Lee KK, Rhee SG, and Yu DY. Peroxiredoxin II is essential for sustaining life span of erythrocytes in mice. *Blood* 101: 5033–5038, 2003.
23. Low FM, Hampton MB, Peskin AV, and Winterbourn CC. Peroxiredoxin 2 functions as a noncatalytic scavenger of low-level hydrogen peroxide in the erythrocyte. *Blood* 109: 2611–2617, 2007.
24. Low FM, Hampton MB, and Winterbourn CC. Peroxiredoxin 2 and peroxide metabolism in the erythrocyte. *Antioxid Redox Signal* 10: 1621–1630, 2008.
25. Ma S, Caprioli RM, Hill KE, and Burk RF. Loss of selenium from selenoproteins: conversion of selenocysteine to dehydroalanine *in vitro*. *J Am Soc Mass Spectrom* 14: 593–600, 2003.
26. Margoliash E, Novogrodsky A, and Schejter A. Irreversible reaction of 3-amino-1:2:4-triazole and related inhibitors with the protein of catalase. *Biochem J* 74: 339–348, 1960.
27. Marzocchi B, Ciccoli L, Tani C, Leoncini S, Rossi V, Bini L, Perrone S, and Buonocore G. Hypoxia-induced post-translational changes in red blood cell protein map of newborns. *Pediatr Res* 58: 660–665, 2005.
28. Moore RB, Mankad MV, Shriver SK, Mankad VN, and Plishker GA. Reconstitution of Ca(2+)-dependent K⁺ transport in erythrocyte membrane vesicles requires a cytoplasmic protein. *J Biol Chem* 266: 18964–18968, 1991.
29. Ninfali P, Palma F, Baronciani L, and Piacentini G. Glucose-6-phosphate dehydrogenase activity and protein turnover in erythroblasts separated by velocity sedimentation at unit gravity and Percoll gradient centrifugation. *Mol Cell Biochem* 106: 151–160, 1991.
30. Palacios O and Lobinski R. Investigation of the stability of selenoproteins during storage of human serum by size-exclusion LC-ICP-MS. *Talanta* 71: 1813–1816, 2007.
31. Peskin AV, Low FM, Paton LN, Maghzal GJ, Hampton MB, and Winterbourn CC. The high reactivity of peroxiredoxin 2 with H₂O₂ is not reflected in its reaction with other oxidants and thiol reagents. *J Biol Chem* 282: 11885–11892, 2007.
32. Pigeolet E, Corbisier P, Houbion A, Lambert D, Michiels C, Raes M, Zachary MD, and Remacle J. Glutathione peroxidase, superoxide dismutase, and catalase inactivation by peroxides and oxygen derived free radicals. *Mech Ageing Dev* 51: 283–297, 1990.
33. Rhee SG, Kang SW, Chang TS, Jeong W, and Kim K. Peroxiredoxin, a novel family of peroxidases. *IUBMB Life* 52: 35–41, 2001.
34. Rifkind JM, Ramasamy S, Manoharan PT, Nagababu E, and Mohanty JG. Redox reactions of hemoglobin. *Antioxid Redox Signal* 6: 657–666, 2004.
35. Rotruck JT, Pope AL, Ganther HE, Swanson AB, Hafeman DG, and Hoekstra WG. Selenium: Biochemical role as a component of glutathione peroxidase. *Science* 179: 588–590, 1973.
36. Rundlof AK and Arner ES. Regulation of the mammalian selenoprotein thioredoxin reductase 1 in relation to cellular phenotype, growth, and signaling events. *Antioxid Redox Signal* 6: 41–52, 2004.
37. Salvo GP, Caprari P, Samoggia P, Mariani G, and Salvati AM. Human erythrocyte separation according to age on a discontinuous "Percoll" density gradient. *Clin Chim Acta* 122: 293–300, 1982.
38. Schnabel R, Lackner KJ, Rupprecht HJ, Espinola-Klein C, Torzewski M, Lubos E, Bickel C, Cambien F, Tiret L, Munzel T, and Blankenberg S. Glutathione peroxidase-1 and homocysteine for cardiovascular risk prediction: Results from the AtheroGene study. *J Am Coll Cardiol* 45: 1631–1637, 2005.
39. Seo J, Jeong J, Kim YM, Hwang N, Paek E, and Lee KJ. Strategy for comprehensive identification of post-translational modifications in cellular proteins, including low abundant modifications: application to glyceraldehyde-3-phosphate dehydrogenase. *J Proteome Res* 7: 587–602, 2008.
40. Singh H, Purnell E, and Smith C. Mechanistic study on aniline-induced erythrocyte toxicity. *Arh Hig Rada Toksikol* 58: 275–285, 2007.
41. Wendel A, Pilz W, Ladenstein R, Sawatzki G, and Weser U. Substrate-induced redox change of selenium in glutathione peroxidase studied by x-ray photoelectron spectroscopy. *Biochim Biophys Acta* 377: 211–215, 1975.
42. Winterbourn CC. Free-radical production and oxidative reactions of hemoglobin. *Environ Health Perspect* 64: 321–330, 1985.
43. Winterbourn CC, McGrath BM, and Carrell RW. Reactions involving superoxide and normal and unstable haemoglobins. *Biochem J* 155: 493–502, 1976.
44. Winterbourn CC and Stern A. Human red cells scavenge extracellular hydrogen peroxide and inhibit formation of hypochlorous acid and hydroxyl radical. *J Clin Invest* 80: 1486–1491, 1987.
45. Wolff SS. Ferrous ion oxidation in presence of ferric ion indicator xylenol orange for measurement of hydroperoxides. *Meth Enzymol* 233: 182–189, 1994.
46. Woo HA, Chae HZ, Hwang SC, Yang KS, Kang SW, Kim K, and Rhee SG. Reversing the inactivation of peroxiredoxins caused by cysteine sulfinic acid formation. *Science* 300: 653–656, 2003.
47. Woo HA, Jeong W, Chang TS, Park KJ, Park SJ, Yang JS, and Rhee SG. Reduction of cysteine sulfinic acid by sulfiredoxin is specific to 2-cys peroxiredoxins. *J Biol Chem* 280: 3125–3128, 2005.
48. Yang KS, Kang SW, Woo HA, Hwang SC, Chae HZ, Kim K, and Rhee SG. Inactivation of human peroxiredoxin I during catalysis as the result of the oxidation of the catalytic site cysteine to cysteine-sulfinic acid. *J Biol Chem* 277: 38029–38036, 2002.

Address correspondence to:

Sue Goo Rhee
Division of Life and Pharmaceutical Sciences
Ewha Womans University
11-1 Daehyun-dong, Seodaemun-gu
Seoul 120-750
Korea

E-mail: rheesg@ewha.ac.kr

Date of first submission to ARS Central, June 4, 2009; date of final revised submission, October 27, 2009; date of acceptance, October 30, 2009.

Abbreviations Used

3-AT = 3-amino-1,2,4-triazole
BIAM = *N*-(biotinoyl)-*N*-9'(iodoacetyl)
ethylenediamine
DHA = dehydroalanine
DMEM = Dulbecco's modified Eagle's medium
DMF = *N,N*-dimethylformamide
DTT = dithiothreitol
FOX = ferrous oxidation of xylenol orange
G6PDH = glucose-6-phosphate dehydrogenase
GAPDH = glyceraldehyde-3-phosphate
dehydrogenase
GO = glucose oxidase
GPx = glutathione peroxidase
GSH = glutathione
Hb = hemoglobin
HEL92.9 = human erythroblastic leukemia
LC-ESI-Q-TOF = liquid chromatography-electrospray
ionization-quadrupole time-of-flight
MALDI-TOF = matrix-assisted laser desorption-ionization
time-of-flight
MS = mass spectrometry
MS/MS = tandem mass spectrometry
Prxs = peroxiredoxins
ROS = reactive oxygen species
Sec = selenocysteine
Srx = sulfiredoxin
Trx = thioredoxin
TrxR = thioredoxin reductase

This article has been cited by:

1. Prof. Rodrigo Soares Fortunato , Mr. William Braga , Mr. Victor Ortenzi , Mr. Deivid Rodrigues , Dr. Bruno Moulin Andrade , Mr. Leandro Miranda Alves , Edson Rondinelli , Dr. Corinne Dupuy , Dr. Andrea Claudia Freitas Ferreira , Prof. Denise Pires de Carvalho MD, DSc . SEXUAL DIMORPHISM OF THYROID REACTIVE OXYGEN SPECIES PRODUCTION DUE TO HIGHER NOX4 EXPRESSION IN FEMALE THYROID. *Thyroid* **0**:ja. . [[Abstract](#)] [[Full Text PDF](#)] [[Full Text PDF with Links](#)]
2. Aldwin Suryo Rahmanto, David I. Pattison, Michael J. Davies. 2012. Photo-oxidation-induced inactivation of the selenium-containing protective enzymes thioredoxin reductase and glutathione peroxidase. *Free Radical Biology and Medicine* **53**:6, 1308-1316. [[CrossRef](#)]
3. David I. Pattison, Michael J. Davies, Clare L. Hawkins. 2012. Reactions and reactivity of myeloperoxidase-derived oxidants: Differential biological effects of hypochlorous and hypothiocyanous acids. *Free Radical Research* **46**:8, 975-995. [[CrossRef](#)]
4. Weixun Li, Jaya Bandyopadhyay, Hyun Sook Hwaang, Byung-Jae Park, Jeong Hoon Cho, Jin Il Lee, Joohong Ahnn, Sun-Kyung Lee. 2012. Two thioredoxin reductases, trxr-1 and trxr-2, have differential physiological roles in *Caenorhabditis elegans*. *Molecules and Cells* **34**:2, 209-218. [[CrossRef](#)]
5. Diane E. Handy , Joseph Loscalzo . 2012. Redox Regulation of Mitochondrial Function. *Antioxidants & Redox Signaling* **16**:11, 1323-1367. [[Abstract](#)] [[Full Text HTML](#)] [[Full Text PDF](#)] [[Full Text PDF with Links](#)]
6. Michael P. Murphy . 2012. Mitochondrial Thiols in Antioxidant Protection and Redox Signaling: Distinct Roles for Glutathionylation and Other Thiol Modifications. *Antioxidants & Redox Signaling* **16**:6, 476-495. [[Abstract](#)] [[Full Text HTML](#)] [[Full Text PDF](#)] [[Full Text PDF with Links](#)]
7. Ho Zoon Chae , Hammou Oubrahim , Ji Won Park , Sue Goo Rhee , P. Boon Chock . 2012. Protein Glutathionylation in the Regulation of Peroxiredoxins: A Family of Thiol-Specific Peroxidases That Function As Antioxidants, Molecular Chaperones, and Signal Modulators. *Antioxidants & Redox Signaling* **16**:6, 506-523. [[Abstract](#)] [[Full Text HTML](#)] [[Full Text PDF](#)] [[Full Text PDF with Links](#)]
8. Christian Brinkmann, Jenny Blossfeld, Martin Pesch, Bastian Krone, Kathrin Wiesiollek, Dario Capin, Georgina Montiel, Martin Hellmich, Wilhelm Bloch, Klara Brixius. 2011. Lipid-peroxidation and peroxiredoxin-overoxidation in the erythrocytes of non-insulin-dependent type 2 diabetic men during acute exercise. *European Journal of Applied Physiology* . [[CrossRef](#)]
9. Edith Lubos , Joseph Loscalzo , Diane E. Handy . 2011. Glutathione Peroxidase-1 in Health and Disease: From Molecular Mechanisms to Therapeutic Opportunities. *Antioxidants & Redox Signaling* **15**:7, 1957-1997. [[Abstract](#)] [[Full Text HTML](#)] [[Full Text PDF](#)] [[Full Text PDF with Links](#)]
10. Samir Mandal, Sudip Mukherjee, Kaustav Dutta Chowdhury, Avik Sarkar, Kankana Basu, Soumosish Paul, Debasish Karmakar, Mahasweta Chatterjee, Tuli Biswas, Gobinda Chandra Sadhukhan, Gargi Sen. 2011. S-allyl cysteine in combination with clotrimazole downregulates Fas induced apoptotic events in erythrocytes of mice exposed to lead. *Biochimica et Biophysica Acta (BBA) - General Subjects* . [[CrossRef](#)]
11. Ojia Skaff, David Pattison, Philip Morgan, Rushad Bachana, Vimal Jain, K. Priyadarsini, Michael Davies. 2011. Selenium-containing amino acids are major targets for myeloperoxidase-derived hypothiocyanous acid: determination of absolute rate constants and implications for biological damage. *Biochemical Journal* . [[CrossRef](#)]
12. Arthur JL Cooper, John T Pinto, Patrick S Callery. 2011. Reversible and irreversible protein glutathionylation: biological and clinical aspects. *Expert Opinion on Drug Metabolism & Toxicology* **7**:7, 891-910. [[CrossRef](#)]
13. Goedeke Roos, Joris Messens. 2011. Protein sulfenic acid formation: From cellular damage to redox regulation. *Free Radical Biology and Medicine* **51**:2, 314-326. [[CrossRef](#)]
14. Shi Kui Wang, Jeremy D. Weaver, Sheng Zhang, Xin Gen Lei. 2011. Knockout of SOD1 promotes conversion of selenocysteine to dehydroalanine in murine hepatic GPX1 protein. *Free Radical Biology and Medicine* **51**:1, 197-204. [[CrossRef](#)]
15. John S. O'Neill, Akhilesh B. Reddy. 2011. Circadian clocks in human red blood cells. *Nature* **469**:7331, 498-503. [[CrossRef](#)]
16. P. A. Tyurin-Kuzmin, K. M. Agaronyan, Ya. I. Morozov, N. M. Mishina, V. V. Belousov, A. V. Vorotnikov. 2010. NADPH oxidase controls EGF-induced proliferation via an ERK1/2-independent mechanism. *Biophysics* **55**:6, 959-965. [[CrossRef](#)]
17. Chun-Seok Cho , Gregory J. Kato , Seung Ha Yang , Sung Won Bae , Jong Seo Lee , Mark T. Gladwin , Sue Goo Rhee . 2010. Hydroxyurea-Induced Expression of Glutathione Peroxidase 1 in Red Blood Cells of Individuals with Sickle Cell Anemia. *Antioxidants & Redox Signaling* **13**:1, 1-11. [[Abstract](#)] [[Full Text HTML](#)] [[Full Text PDF](#)] [[Full Text PDF with Links](#)] [[Supplemental material](#)]